PCCP

Accepted Manuscript

ROYAL SOCIETY OF CHEMISTRY

www.rsc.org/pccp

Journal Name

RSCPublishing

ARTICLE

Modelling Analysis of the Structure and Porosity of Covalent Triazine-Based Frameworks

Cite this: DOI: 10.1039/xoxx00000x

Christian Reece[a], David J. Willock[a] and Abbie Trewin[b*]

Received ooth January 2012,
Accepted ooth January 2012

DOI: 10.1039/xoxx00000x

www.rsc.org/

Varying degrees of order have been found experimentally for a series of covalent triazine-based frameworks (CTFs) when synthesised under different reaction conditions. Here, we use molecular modelling to discuss the potential origins of this structural order by analysis of the node and strut building blocks. We use a combination of small model structures based on DFT optimised monomer units and more extended simulations using automated structure growth and molecular dynamics to discuss the influence of the strut structure on the local crystallinity of these materials.

Introduction

Materials that exhibit microporosity such as metal-organic frameworks (MOFs)[1], covalent organic frameworks (COFs)[2], and microporous organic polymers (MOPs) have important potential applications for gas adsorption, heterogeneous catalysis, and chemical separations.[3] Crystalline COFs and MOFs can exhibit ultra high surface areas (Brunauer Emmett Teller (BET) surface areas over 6000 m^2/g)[5] with good thermal stabilities reported, although some studies suggest chemical decomposition, for example, of COF-1 in air. MOPs, by contrast, have been shown to be very robust with good physicochemical stabilities, for example towards water. A number of different MOPs have been developed showing the wide synthetic diversity that is available. These include hyper-crosslinked polymers (HCPs),[6] porous aromatic frameworks (PAFs),[7] conjugated microporous polymers (CMPs)[8] and polymers of intrinsic microporosity (PIMs).[9] Covalent triazine-based frameworks (CTFs)[10] are known to be extremely stable but, as yet, do not exhibit the ultra high surface areas observed for 3-dimensional COFs, MOFs, and PAFs. High surface area CTFs, up to 3000 m^2/g apparent BET surface area in some cases, have been reported using ionothermal synthesis with molten $ZnCl_2$ as the solvent and catalyst at high temperatures of 400-700 °C.[10-11] However, these harsh conditions and the long reaction times required limit the monomer choice and hence the practical applications. Such harsh conditions can also lead to significant nitrogen loss from the materials.

Recently, a series of CTFs with different monomer topologies were reported synthesised using trifluoromethanesulfonic acid (TFMS) as the catalyst under both room temperature and microwave-assisted conditions P1 to P6, and P1M to P6M, respectively.[4] These mild synthetic conditions will allow for a wide range of functional group diversity to be incorporated that were previously intolerant to harsh ionothermal conditions. In some cases, the structural and gas uptake properties of the CTFs differed significantly between the two different synthesis conditions. For example, the CTFs synthesised using microwave heating had lower surface areas than those synthesised at room temperature, in some cases the surface area was reduced by 56 %. Furthermore, a number of the CTFs synthesised using microwave heating also exhibited some limited evidence of crystallinity. This was attributed speculatively to the combination of increased pressure in the microwave environment and the acid catalyst facilitating the making and breaking of bonds, and hence promoting the thermodynamic product.

A common strategy for designing microporous materials with high surface areas is to use monomers and chemistry that aim towards materials with high degrees of order,[12] such as MOFs or COFs, or those that have short rigid linkers that inhibit network interpenetration, such as certain CMPs and PAFs.[13] For the series of CMP materials that are topologically similar to CTFs, we have previously observed the trend that longer struts are able to pack more efficiently, resulting in higher density materials with a lower surface area.[8a, 13b, 14] The inherent flexibility of CMP structures with longer struts is demonstrated by the bending of struts out of plane of the nodes, the bending of the struts themselves, the broad range of values observed in the dihedral angle between struts on adjacent nodes, and the in-plane deviation of the angle between struts from the hypothetical ideal. NCMP-0, with the shortest strut length of 0.69 nm, exhibits the highest surface area of the reported CMP series (1108 m^2/g). Similarly, P5, with the shortest node-to-node distance, has the highest BET surface area (960 m^2/g) in contrast to P1 (2 m^2/g), which has a similarly short node-to-node distance. This apparent contradiction raises some interesting questions about the design strategy for these types of microporous material. It is important to understand the role of structural flexibility on the degree of long-range order of

the resulting topology and its influence on surface area properties.

Herein, atomistic models of the CTF materials P1 to P5, are presented for structural analysis, focussing on the structural degrees of freedom available and their influence on the structural topologies obtained, and hence rationalising the porous properties.

Results

Models were generated using the *Material Studio Modelling 5.0* package (Accelrys Inc. San Diego, CA, 2009) and the geometry optimised using the *Forcite* module and PCFF forcefield. The geometry of node-strut models consisting of two nodes and the respective linking strut were further optimised using NWChem 6.1 with the 6-311G basis set and B3LYP functional and incorporating the Grimme dispersion correction.[15]

Figure 1 shows the monomer building units and the resulting node and strut with optimised geometry, details described in ESI section 2. Table 1 shows the node-to-node distances obtained from the node-strut models and the nodal dimensionality, a description of these topological analysis measurements can be found in ESI section 3.

The flexibility or rigidity of a network can be directly related to the combination of nodal dimensionality, nodal flexibility, and strut length. Nodes that are highly 3-dimensional and flexible instigate a greater degree of randomness within the network's 3-D structure. Combining these flexible 3-dimensional nodes with short linkers that are unable to interpenetrate, and hence pack inefficiently, will result in a more porous network structure. Conversely, combining flexible 3-dimensional nodes with longer flexible linkers will facilitate efficient network packing, thereby reducing the porosity.

Nodes that are 2-dimensional and rigid would be expected to approximate towards the idealised crystalline repeating unit. The degree to which this occurs is dependent upon the flexibility of the combined linker. For P1 to P5, with the combination of 1-D linkers and 2-D nodes, a hexagonal sheet-like network would be expected, which can stack to give layers that are directly on top of each other or are offset. Reversible chemistry is widely believed to be key to the formation of ordered networks so that faults and misalignments within the network can be corrected or 'self healed', and hence something close to the global thermodynamic product is achieved. For chemistry that is not easily reversible, such as in this triazine case, it may be that the amorphous network nonetheless shares features in common with the idealised planar sheet-like crystalline structure such as hexagonal rings or layer stacking motifs resulting in a lamellar sheet-like structure. The porosity of these materials would also be expected to be a function of the linker size; but in this case shorter linkers would give smaller ideal hexagonal rings that would be more easily blocked by nodes and struts above and below leading to less connected volume and hence lower porosity. Whereas longer more flexible linkers introduce 3-dimensionality to the network, instigating randomness within the structure and therefore reduce the efficiency of the network packing.

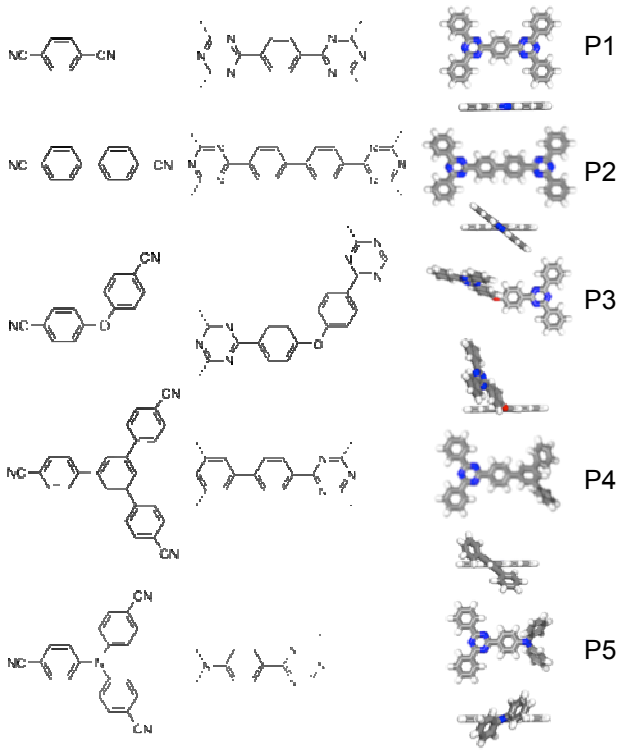

Figure 1. The building blocks for the series of CTF type polymers P1 to P6 that are synthesised at room temperature and using TFMS as a catalyst. Left: The monomer building units. Right: Representative structure of the node and strut of the respective CTF polymer.

Table 1: Showing the experimentally obtained physical and porosity properties of the five CTF systems, P1 to P5 with the geometrical measurements obtained from atomistic models of their respective node-strut models.

Polymer	SA_{BET} (m^2/g) [a]	Node-to-Node (nm) [b]	In-plane angle (°)[c]	Out of-plane angle (°)[d]	Nodal dimension-ality (°)[e]
P1	2	0.84	120	180	0.6
P2	776	1.27	120	178	39.0
P3	571	1.24	120	153	85.0
P4	867	0.85	120	179	41.0
P5	960	0.70	120	179	29.0

[a] From ref 11, synthesised using TFMS catalyst and room temperature conditions. [b c d e] Description found in ESI section 3.

To test the hypotheses outlined above for polymers constructed from 2-D nodes and 1-D linkers, small cluster models of P1 to P5 were constructed, three for each respective system. The clusters were built sequentially by adding the DFT-optimised node-strut model units to a DFT-optimised node-strut core pair,

saturating all attachment points at each layer addition. A total of three layers were added to form the cluster. Each node-strut model pair is added as part of a motion group, fixing its internal structure but allowing bonds between motion groups to be optimised. After each layer addition the geometry of the cluster is optimised using the *Forcite* module and PCFF force field.[16] Finally, the motion groups are removed and the structure is fully optimised. The resulting clusters are intended as simplified samples of the local kinetic network product from which we can infer structural trends. Of course, there are many ways in which a particular cluster could be formed, and these models are not intended to be definitive, but rather to explore structural trends as a precursor to future studies. Three clusters for each polymer were independently generated, an example of each is shown in Figure 2, computational details and cluster analysis are described in ESI section 3 and 4 respectively, and clusters are shown in ESI section 5. Cluster dimension analyses for the three clusters of each polymer are reported in full in Table. ESI.1. It should be noted that these cluster models are not intended to be representative of the polymer in its true packed form.

The small clusters of P1 show features in common with the idealised hexagonal layer sheet, such as partial ring formation and layer stacking. The idealised structure is broken by imperfections in the layer formation, which introduces disorder in the structure and leads to a structure that exhibits some limited degree of local order, but is considered to be largely amorphous. This is reflected in the shape and dimension of the cluster, which is flat and oval. It has an average cluster diameter of 86 Å and a cluster height of 21 Å. Full ring formation is not allowed in the cluster generation methodology. However, the 2-dimensionality of the node-strut model for P1 leads to a high number of partial ring formations within the clusters suggesting an increased likelihood of full ring formation in the polymer structure. The clusters of P2, with its greater node-node distance, has a greater average cluster diameter of 111 Å and has an average cluster height of 77 Å being closer to a spherical cluster and reflecting its greater nodal dimensionality. Some partial ring formation and partial layer stacking can be observed. P3 forms roughly spherical clusters with an average diameter of 93 Å and an average cluster height of 91 Å. No evidence of partial ring formation or layer stacking is observed within the P3 clusters. Interpenetration of the cluster network is observed for P2 and P3. The P4 clusters have a similar average diameter (80 Å) as P1, as expected from the similar node-to-node distance, but has a greater cluster height of 62 Å due to its greater nodal dimensionality (41°) compared to the P1 nodal dimensionality (0.6°), which introduces 3-dimensionality to the cluster. Some layer stacking can be observed within the P4 clusters. P5 has the shortest node-to-node distance. This is reflected in the small average cluster diameter and height of 62 Å and 59 Å respectively. No evidence of partial ring formation or layer stacking is evident with the cluster structure and no network interpenetration is observed.

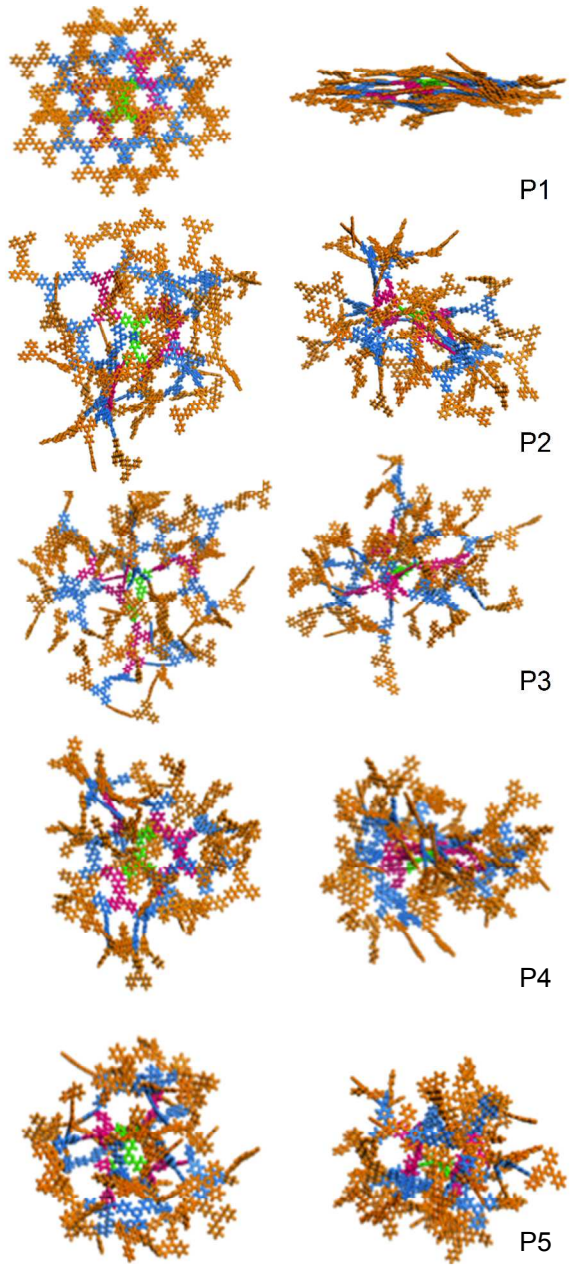

Figure 2. Small clusters of P1 to P5, top view (left) and side view (right). The clusters were generated by step-wise addition of building units to a central building unit based on the respective DFT optimised node-strut pairs. The central building unit is shown in green, the second set of building units are shown in pink, third in blue, and fourth in orange.

Structural analysis of the small CTF clusters reveals that the P1 clusters have a high degree of partial ring formation and a high degree of layer stacking. The P2 clusters show some partial ring formation and some layer stacking. The clusters of P4 exhibit some layer stacking but no partial ring formation is observed within the clusters. The clusters of P3 and P5 exhibit no partial ring formation or layer stacking. From this analysis, one might expect to observe some experimental evidence of order

resulting from the layer stacking and partial ring formation motif. Peaks suggesting some preferential ordering have been observed in the PXRDs of P1, P2, and P4 synthesised under microwave heating conditions.[4] Ionothermal synthesis with molten $ZnCl_2$ as the solvent and catalyst at high temperatures of 400-700 °C of CTF-1, a CTF with the same node-strut as P1, resulted in a material with high surface area (791 m^2/g) and some evidence of long-range order.[10] The observed peaks in the PXRD compared well to the calculated PXRD for an idealised sheet-like model although peak broadening suggested limited long-range order.[10]

To further test the hypothesis, large cluster models of P1 to P5 were built following an automated procedure using the Zebedde program and then molecular dynamic (MD) simulation was undertaken.[17] For each system separate calculations were carried out starting from 3,6,9,12 and 15 initial triazine seed molecules. Each seed molecule will give rise to a distinct molecular network so that by varying the number of seeds we can consider the effect of interpenetration of networks. The triazine seed molecules were placed in a cubic periodic repeat unit 5.0 nm on a side. The H atoms of the triazine were denoted "HA" and H atoms at the polymer forming positions on each of the PX (X=1,5) monomers were labeled "HB". For each building run one of the PX and the triazine molecule were included in a fragment library and additions made to the growing polymer by picking from this library at random with equal probability. Additions to the current structure followed the rule that new bonds could only form by elimination of one HA and one HB each chosen at random from either the current structure or the molecule from the fragment library. During the growth process additional Monte Carlo (MC) moves involving random bond twists and whole molecule translations/rotations were included. After an addition to the growing structure the probability of testing was set to 0.5% so that a significant number of MC moves were attempted after each new build action. The total build sequence consisted of 5×10^6 build/MC move attempts at a simulation temperature of 350 K. The system energy was calculated using the PCFF forcefield.

The growth procedure produced large cluster models of each CTF material consisting of 100-200 triazine units connected to form inter-penetrating networks. In general the average density of the structures produced increased with the number of seed molecules used. For example, with 3 seeds a system density of 0.25 g cm^{-3} was achieved for P1 and this increased to 0.37 g cm^{-3} with 15 initial seeds. However, the individual CTF network sizes decreased with seed number so that the average number of triazine units per molecule with 3 seeds was 38.3 whereas using 15 seeds this average fell to 11,1. Test calculations with 18 seeds gave a lower average and some single triazine molecules remaining at the end of the run, so that the growth process appears to become more difficult beyond a seed number of 15. The structures produced were then used as inputs to microcanonical (NVE) Molecular dynamics

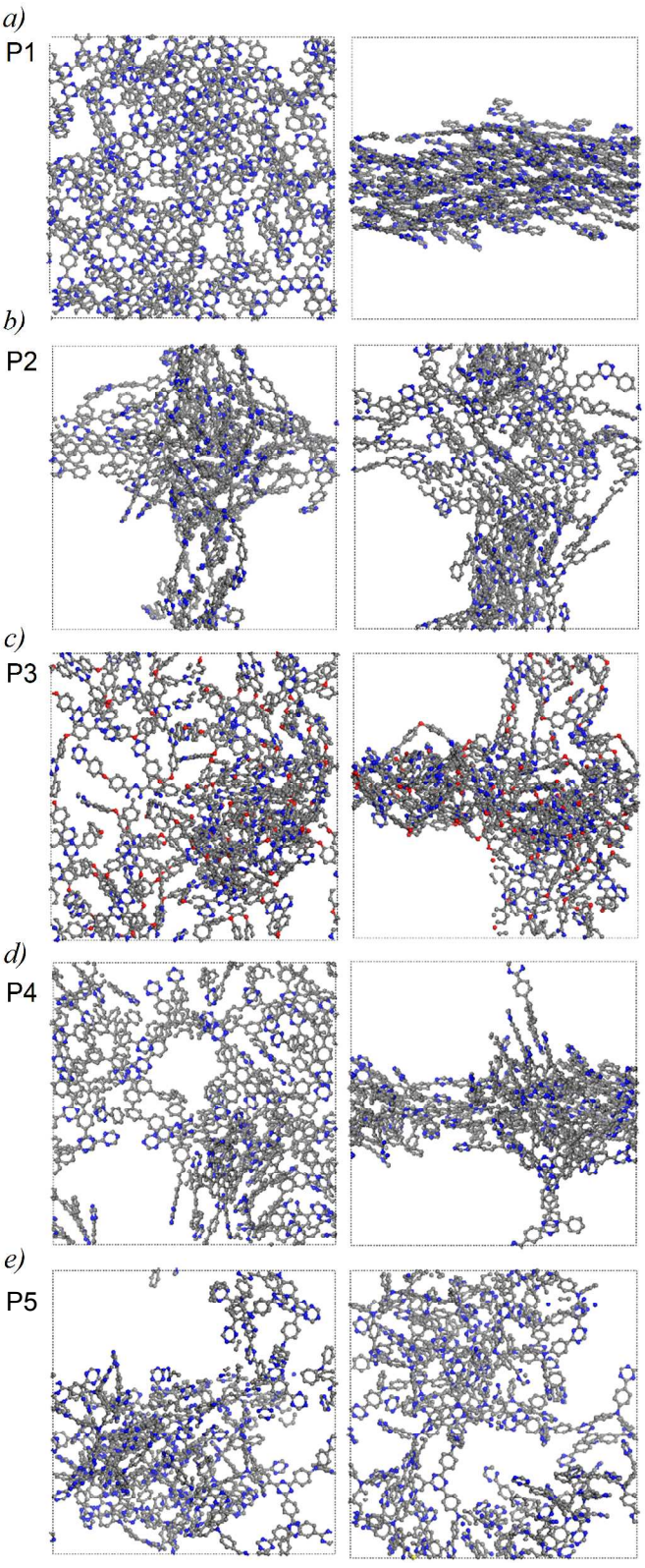

Figure 3. Final frames from 1 ns NVE simulations of the Zebedde constructed models with 15 seed molecules for *a*) P1, *b*) P2, *c*) P3, *d*) P4 and *e*) P5. In each case two perpendicular views are shown and a black dotted line is given for the periodic boundaries of the simulation.

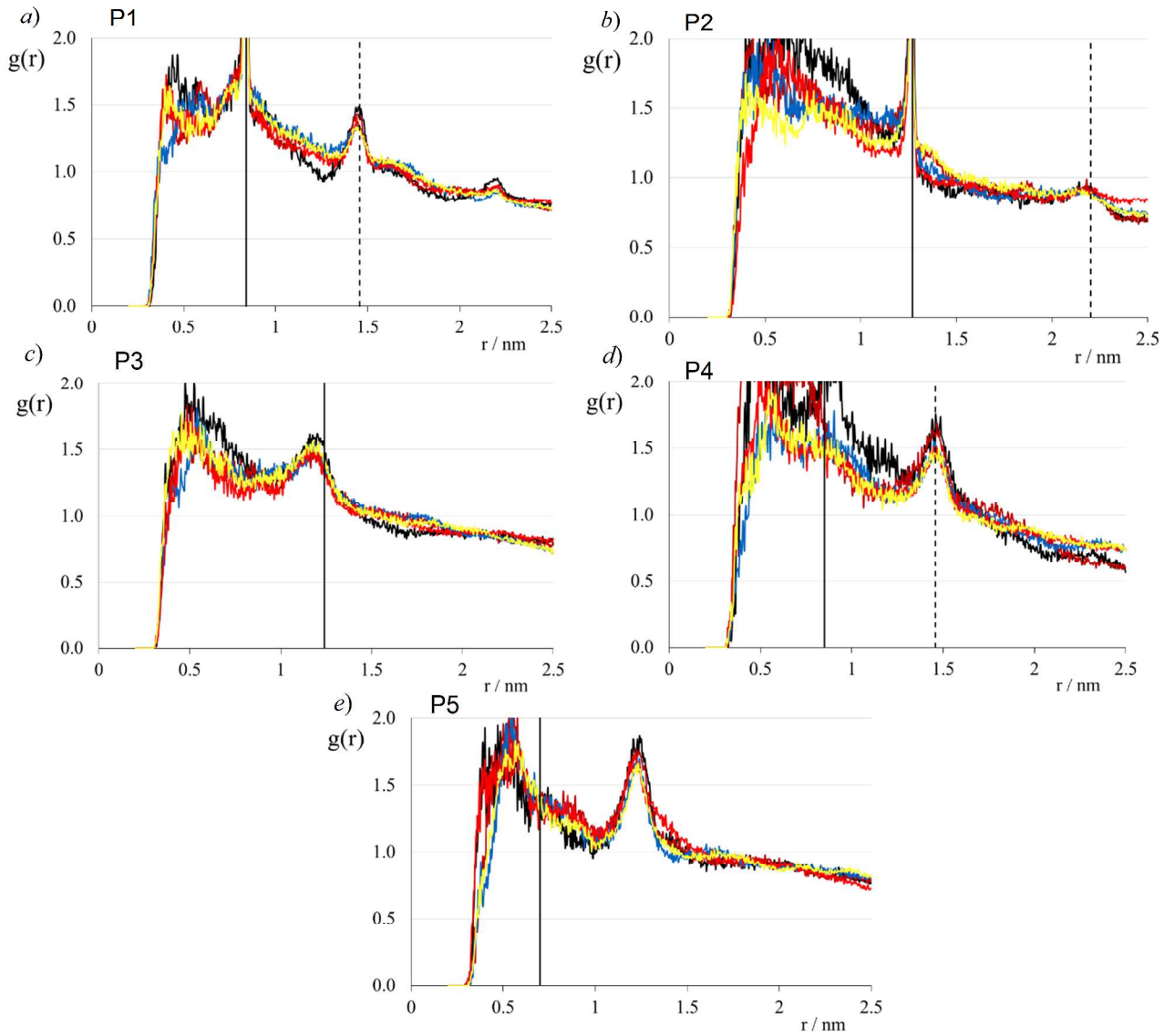

Figure 4. Radial distribution functions from 1 ns MD trajectories for the CTF networks for *a*) P1, *b*) P2, *c*) P3, *d*) P4 and *e*) P5. In each case lines are coloured according to the number of seeds used with black: 3, brown: 6, blue: 9, red: 12 and yellow: 15. The vertical solid line indicates the node to node distance given in table 1, the vertical dashed line indicates the periodicity identified from PXRD for P1, P2 and P4 in reference 4.

(MD) simulations at a temperature of 300 K using the DLPOLY code.[18] After 50 ps equilibration the MD runs were used to produce 1 ns simulations with the trajectory sampled every 2.5 ps.

Figure 3 shows snapshots from the end of the MD simulations for each of the CTF systems based on the structures produced using 15 seed triazine molecules. For the P1 network a clear layered structure with the aromatic ring systems of the 15 individual molecules forming roughly planar sheets can be seen (Figure 3*a*). The layer structure itself shows a fairly uniform density. Figure 3b shows two views of the P2 structure, which also shows a tendency to form a layered material but not so well defined as for P1. There are also a number of sections of individual molecules that have grown in a perpendicular direction forming a link between periodic images of the main sheet and the sheet itself has notable voids present. For P3 (Figure 3c) there is also dense layer region with a few molecules constructed in the perpendicular direction, however there is no view of this system from which layers can be discerned in the structure. In the snapshot for P4 (Figure 3d) we see a return to a layered structure with a similar appearance to P2. Finally Figure 3e shows the structure of P5 which has a much more globular appearance than the other networks with no particular layering direction observable.

To further assess the structures produced from the MD run and to check on the degree of order in each system the radial distribution function (g(r)) based on the triazine ring centroids was generated for each of the 1 ns MD trajectories. These are shown in Figure 4 and in more detail in ESI section 7.

In each case there is a distinct peak for the corresponding triazine node-node distance given in table 1 from the cluster models discussed earlier and in ESI section 6. For P1 and P2

these are very sharp features and the corresponding peaks go as high as g(r)=8. This is a consequence of the rigid linkers used in these cases, which limits the range of node-node distances which can be sampled during the MD run. Longer range correlations lead to broader lower peaks and to make easier comparison of these we have restricted the g(r) plot range to 2 for all the networks shown. We note that the node-node distance quoted in table 1 for P4 and P5 refer to the phenyl and N atom of the linker to triazine centroid distance respectively since these form nodes within the respective framework. However, the g(r) plots are for triazine centroids only, measuring the inter-centroid distance in the smaller models does give a value of 1.47 nm and 1.27 nm respectively, in good agreement with the first peaks in the g(r) for Figure 4d and 4e. We have noted from Figure 3 that all simulations contain significant void space so that the distribution of atoms is not as even as expected in the g(r) normalization. This leads to high initial values (around 0.5 nm) in each plot since at this range the effective centroid density is higher than expected for a uniform distribution. We also note that the g(r) values tend to less than 1 at long range since for this part of the data the sampling sphere around each centroid will include a significant amount of void space. The g(r) plots for 3,6,9,12 and 15 seed runs are overlayed for each polymer. In general there are only small variations between the different seed numbers used indicating that the network structures produced by the five distinct simulations are consistent with one another.

From the g(r) plot for P1 we see a distinct peak at around 1.45 nm. The vertical dashed line in the plot shows that this correlates well with the powder X-ray diffraction (PXRD) result reported by Cooper and co-workers[4] who found a sharp peak corresponding to a periodicity of 1.4574 nm for this material. A second peak at 2.21 nm evident in Figure 4a is also consistent with the third neighbor distance in neighbouring hexagonal units in a network as explained in section 8 of the ESI. The ESI also shows that the third order neighbor within the same hexagon should occur at 1.68 nm and there does appear to be a broad feature in the g(r) at this distance. Inspection of the trajectory shows that, although local order is well defined, torsional motion tends to lead to variations in inter-centroid distances at this separation, and geometry dictates that the intra-hexagonal third neighbor distance is more strongly influenced than that for adjacent hexagonal sections of the network. The larger, rigid linker used in P2 was also found to lead to some periodicity in the PXRD experiments. The repeat unit of 2.2016 nm found experimentally also matches with the second peak in the corresponding g(r) plot (Figure 4*b*). In contrast, after the initial peak due to the effect of non-uniform density in these simulations, Figure 4*c* shows only a single peak for the P3 system, which corresponds to the nearest neighbor triazine node-node distance. No experimental PXRD for this material has been reported and our simulations indicate that this is because the linker leads to a truly amorpohous network. The P4 system has a reported repeat distance identical to P1 from PXRD. Again our MD simulations show a peak at the corresponding separation for the triazine node-node distance (see ESI section 7) in the network. The P5 simulations only show the single peak for nearest neighbor triazine nodes that we discussed for P3, so again we conclude that this system is largely amorphous.

Considering the structural properties of the CTF clusters with respect to their porosity properties, it is possible to elucidate the relative influence of the node and linker structure on the cluster structure and resulting porosity properties. P1 and P2 share a common node, but P1 has a shorter, more rigid linker than P2, which has a twist in the biphenyl linking group and a nodal dimensionality of 39°. P1 is essentially non-porous whereas P2 has a BET surface area of 776 m^2/g. P1 and P4 share the same linker but differ in one node of the P4 dimer being a phenyl group and has a nodal 3-dimensionality of 41°. P1 is non-porous whereas P4 has a BET surface area of 867 m^2/g. P2 also shares a common node with P3 and both have similar node-to-node distance (1.27 nm and 1.24 nm respectively). P3 has a high degree of 3-dimensionality and flexibility to the linking group. This allows it to pack more efficiently and a greater degree of network interpenetration is observed and hence P3 has a comparatively lower BET surface area than P2. P4 and P5 have the same linking group but different asymmetric nodes. The nitrogen atom node of P5 combines both nodal 3-dimensionality and structural flexibility. P5 has a higher BET surface area of 960 m^2/g than P4 with 867 m^2/g.

Conclusions

In summary, we have assessed the structure directing effects of the polymer molecular building block on the resulting simulated structure and porosity properties of a series of CTF polymers. The structure of a single building node-to node unit, a small cluster built in a stepwise manner, and a large randomly built cluster has been assessed.

For the large randomly built cluster we are able to extract structural factors and relate these to experimental data. This has allowed us to identify the origin of evidence for structural order in an otherwise amorphous series of materials. Polymers constructed from very short and rigid linkers with two-dimensional flat nodes result in very well defined repeating distances within the network that are visible in PXRD patterns.

We are further able to formulate some basic rules for relating the nodal dimensionality and node-to-node distance to porosity properties. Increasing the nodal dimensionality and flexibility increases the surface area whereas increasing the node-to-node distance and linker flexibility reduces the surface area. This suggests that the best strategy for maximising the surface area for this class of materials is to have the highest nodal dimensionality and flexibility combined with short rigid linking groups.

Acknowledgement. AT holds a Royal Society Fellowship.

Notes and references

[a] School of Chemistry, Cardiff University, Cardiff, UK, CF10 3AT.

[b] Dept of Chemistry, Lancaster University, Lancaster, UK, LA1 4YB.

Electronic Supplementary Information (ESI) available: CIF files for the node-strut models and cluster models of P1 to P5 (description of files in Supporting Information text document) and computational details for node-to-node models, small clusters and large clusters generated through automated process.

1. (a) Eddaoudi, M.; Moler, D. B.; Li, H.; Chen, B.; Reineke, T. M.; O'Keefe, M.; Yaghi, O. M., Modular chemistry: secondary building units as a basis for the design of highly porous and robust metal-organic carboxylate frameworks. *Acc. Chem. Res.* **2001,** *34*, 319-330; (b) Kitigawa, S.; Kitaura, R.; Noro, S., *Angew. Chem., Int. Ed.* **2004,** *43*, 2334-2375; (c) Han, S. S.; Goddard, W. A., Lithium-Doped Metal-Organic Frameworks for Reversible H2 Storage at Ambient Temperature. *Journal of the American Chemical Society* **2007,** *129* (27), 8422-8423.

2. (a) Côté, A. P.; Benin, A. I.; Ockwig, N. W.; O'Keeffe, M.; Matzger, A. J.; Yaghi, O. M., Porous, crystalline, covalent organic frameworks. *Science* **2005,** *310* (5751), 1166-1170; (b) Hunt, J. R.; Doonan, C. J.; LeVangie, J. D.; Cote, A. P.; Yaghi, O. M., Reticular synthesis of covalent organic borosilicate frameworks,. *J. Am. Chem. Soc.* **2008**, 11872-11873; (c) Cote, A. P.; El-Kaderi, H. M.; Furukawa, H.; Hunt, J. R.; Yaghi, O. M., *J. Am. Chem. Soc.* **2007,** *129*, 12914 - 12915; (d) El-Kaderi, H. M.; Hunt, J. R.; Mendoza-Cortes, J. L.; Cote, A. P.; Taylor, R. E.; O'Keefe, M.; Yaghi, O. M., Designed synthesis of 3D covalent organic frameworks, . *Science* **2007,** *316*, 268-272; (e) Wan, S.; Guo, J.; Kim, J.; Ihee, H.; Jiang, D., A Belt-Shaped, Blue Luminescent, and Semiconducting Covalent Organic Framework, . *Angew. Chem. Int. Ed.* **2008,** *47*, 1-5.

3. (a) Germain, J.; Fréchet, J. M. J.; Svec, F., Nanoporous Polymers for Hydrogen Storage. *Small* **2009,** *5* (10), 1098-1111; (b) Dawson, R.; Cooper, A. I.; Adams, D. J., Nanoporous organic polymer networks. *Progress in Polymer Science* **2012,** *37* (4), 530-563; (c) Barbour, L. J., Crystal porosity and the burden of proof. *Chemical Communications* **2006,** (11), 1163-1168; (d) Cheetham, A. K.; Ferey, G.; Loieau, T., Open-Framework Inorganic Materials. *Angew. Chem. Int. Ed.* **1999,** (38), 3268 - 3292; (e) Jones, J. T. A.; Hasell, T.; Wu, X.; Bacsa, J.; Jelfs, K. E.; Schmidtmann, M.; Chong, S. Y.; Adams, D. J.; Trewin, A.; Schiffman, F.; Cora, F.; Slater, B.; Steiner, A.; Day, G. M.; Cooper, A. I., Modular and predictable assembly of porous organic molecular crystals. *Nature* **2011,** *474* (7351), 367-371.

4. Ren, S.; Bojdys, M. J.; Dawson, R.; Laybourn, A.; Khimyak, Y. Z.; Adams, D. J.; Cooper, A. I., Porous, Fluorescent, Covalent Triazine-Based Frameworks Via Room-Temperature and Microwave-Assisted Synthesis. *Advanced Materials* **2012,** *24* (17), 2357-2361.

5. Furukawa, H.; Ko, N.; Go, Y. B.; Aratani, N.; Choi, S. B.; Choi, E.; Yazaydin, A. O.; Snurr, R. Q.; O'Keeffe, M.; Kim, J.; Yaghi, O. M., Ultrahigh Porosity in Metal-Organic Frameworks. *Science* **2010,** *329* (5990), 424-428.

6. Wood, C. D.; Tan, B.; Trewin, A.; Niu, H.; Bradshaw, D.; Rosseinsky, M. J.; Khimyak, Y. Z.; Campbell, N. L.; Kirk, R.; Stoeckel, E.; Cooper, A. I., Hydrogen Storage in Microporous Hypercrosslinked Organic Polymer Networks,. *Chem. Mat.* **2007,** *19*, 2034-2048.

7. (a) Ben, T.; Ren, H.; Ma, S.; Cao, D.; Lan, J.; Jing, X.; Wang, W.; Xu, J.; Deng, F.; Simmons, J.; Qiu, S.; Zhu, G., Targeted Synthesis of a Porous Aromatic Framework with High Stability and Exceptionally High Surface Area. *Angewandte Chemie International Edition* **2009,** *48* (50), 9457-9460; (b) Trewin, A.; Cooper, A. I., Porous Organic Polymers: Distinction from Disorder? *Angewandte Chemie International Edition* **2010,** *49* (9), 1533-1535.

8. (a) Jiang, J.; Su, F.; Trewin, A.; Wood, C. D.; Campbell, N. L.; Niu, H.; Dickinson, C.; Ganin, A. Y.; Rosseinsky, M. J.; Khimyak, Y. Z.; Cooper, A. I., *Angew. Chem. Int. Ed.* **2007,** *46*, 1 - 5; (b) Weber, J.; Thomas, A., Toward Stable Interfaces in Conjugated Polymers: Microporous Poly(p-phenylene) and Poly(phenyleneethynylene) Based on a Spirobifluorene Building Block. *Journal of the American Chemical Society* **2008,** *130* (20), 6334-6335.

9. McKeown, N. B.; Budd, P. M., Polymers of intrinsic microporosity (PIMs): organic materials for membrane separations, heterogenous catalysis and hydrogen storage. *Chem. Soc. Rev.* **2006,** *35*, 675-683.

10. Kuhn, P.; Antonietti, M.; Thomas, A., *Angew. Chem. Int. Ed.* **2008,** *47*, 3450-3453.

11. (a) Kuhn, P.; Forget, A.; Su, D.; Thomas, A.; Antonietti, M., From Microporous Regular Frameworks to Mesoporous Materials with Ultrahigh Surface Area: Dynamic Reorganization of Porous Polymer Networks. *Journal of the American Chemical Society* **2008,** *130* (40), 13333-13337; (b) Kuhn, P.; Thomas, A.; Antonietti, M., *Macromolecules* **2009,** *42*, 319-326; (c) Bojdys, M. J.; Jeromenok, J.; Thomas, A.; Antonietti, M., Rational Extension of the Family of Layered, Covalent, Triazine-Based Frameworks with Regular Porosity. *Advanced Materials* **2010,** *22* (19), 2202-2205.

12. (a) Trewin, A., Predicting crystalline polyamic acids as precursors to porous polyimides. *CrystEngComm* **2010,** *12* (8), 2315-2317; (b) Trewin, A.; Cooper, A. I., Predicting microporous crystalline polyimides. *CrystEngComm* **2009,** *11* (9), 1819-1822; (c) Jackson, K. T.; Reich, T. E.; El-Kaderi, H. M., Targeted synthesis of a porous borazine-linked covalent organic framework. *Chemical Communications* **2012,** *48* (70), 8823-8825.

13. (a) Trewin, A.; Willock, D. J.; Cooper, A. I., Atomistic Simulation of Micropore Structure, Surface Area, and Gas Sorption Properties for Amorphous Microporous Polymer Networks. *The Journal of Physical Chemistry C* **2008,** *112* (51), 20549-20559; (b) Jiang, J.-X.; Trewin, A.; Su, F.; Wood, C. D.; Niu, H.; Jones, J. T. A.; Khimyak, Y. Z.; Cooper, A. I., Microporous Poly(tri(4-ethynylphenyl)amine) Networks: Synthesis, Properties, and Atomistic Simulation. *Macromolecules* **2009,** *42* (7), 2658-2666.

14. Jiang, J.-X.; Su, F.; Trewin, A.; Wood, C. D.; Niu, H.; Jones, J. T. A.; Khimyak, Y. Z.; Cooper, A. I., Synthetic Control of the Pore Dimension and Surface Area in Conjugated Microporous Polymer and Copolymer Networks. *Journal of the American Chemical Society* **2008,** *130* (24), 7710-7720.

15. (a) Valiev, M.; Bylaska, E. J.; Govind, N.; Kowalski, K.; Straatsma, T. P.; Van Dam, H. J. J.; Wang, D.; Nieplocha, J.; Apra, E.; Windus, T. L.; de Jong, W. A., NWChem: A comprehensive and scalable open-source solution for large scale molecular simulations. *Computer Physics Communications* **2010,** *181* (9), 1477-1489; (b) Grimme, S.; Antony, J.; Ehrlich, S.; Krieg, H., A consistent and accurate ab initio parametrization of density functional dispersion correction (DFT-D) for the 94 elements H-Pu. *The Journal of Chemical Physics* **2010,** *132* (15), 154104-19.

16. Sun, H., Ab initio calculations and force field development for computer simulation of polysilanes. *Macromolecules* **1995,** *28* (3), 701-712.

17. Trewin, A.; Willock, D. J.; Cooper, A. I., *J. Phys. Chem. C.* **2008**, 20549-20559.

18. Todorov, I.; Smith, W.; Trachenko, K.; Dove, M. T., *J. Mater. Chem.* **2006,** *16*, 1611-1618.